Jaffe    Planetary Radio Astronomy

# Thermal emission from major planets

For Jupiter, saturn, opacity is mostly from pressure broadened Ammonia

$$K = 2\pi^2 \mu_0^2 \, \frac{\nu^2 n \alpha}{kT} \, \frac{\Delta\nu_n}{(\nu-\nu_0)^2 + (\Delta\nu)^2} \qquad \Delta\nu = n v_T \sigma_{coll} \approx n$$

~~generally~~ for low freq $\nu < \nu_0$

- $T(\nu)$ given by $\tau = 1 = \int K\,dz$

in adiabatic atmosphere $\quad T = T_c + \beta z \, ; \quad \beta = \frac{\gamma-1}{\gamma}\frac{\mu g}{k}$

$= 4\ \mathrm{K/km}$

$$n = n_c \left(\frac{T}{T_c}\right)^{\frac{1}{\gamma-1}} \; ; \quad \gamma \sim 1.4$$

$$\tau = \beta^{-1}\int_{T_c}^{T} K(T)\,dT = \tau_0 \log\left[\left(\frac{\Delta\nu_{0c}}{\nu_0}\right)^2 \left(\frac{T}{T_c}\right)^{\frac{2}{\gamma-1}} + 1\right] = 1$$

$$\tau_0 \doteq \pi^2 \mu_c^2 \alpha \nu^2 (\gamma-1) n_c / 3k\Delta\nu_c \beta$$

near for lower pressures ($\Delta\nu_c \ll \nu_0$) + temps

$$\left(\frac{T}{T_c}\right) \sim \left[\left(\frac{\nu_0}{\Delta\nu_c}\right)\tau_0^{-\frac{1}{2}}\right]^{\gamma-1} \propto \nu^{-0.4}$$

For high temp $\quad \frac{T}{T_c} = \left(\frac{\nu_0}{\Delta\nu_0}\right)^{+0.4} e^{-\frac{1}{5\tau_0}} \propto e^{-\frac{1}{\nu^2}}$

---

Reasonable agreement for saturn, Jupiter

not for Uranus, Nept

# Rings of Saturn

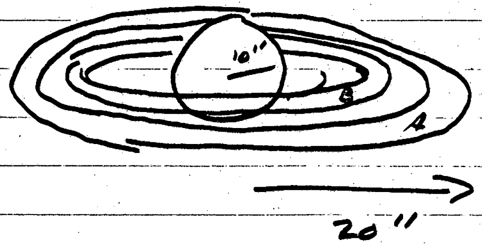

$T_{disk} \sim 170$ K (6 cm)
$T_A \sim 4$ K
$T_B \sim 7$ K
$\tau \sim 1.0$ (0.4 normal)
$T_{IR} \sim 100$ K

radar reflectivity ~ 140 %

$T_B$ scattering ~ 5-6 K for B ring $\Rightarrow \varepsilon > 99\%$

$\varpi$ = single scattering albedo $= \dfrac{Q_s}{Q_s + Q_A} \gtrsim 99.5\%$

$\Rightarrow$ very low loss material ($H_2O$ ice could be metallic)

size $\dfrac{\tau_{radio}}{\tau_{optical}} \approx$ unity, varies slowly with $\lambda$ (?)

$\Rightarrow \dfrac{Q_{ext\ rad}}{Q_{e\ opt}} \approx 1$

typically

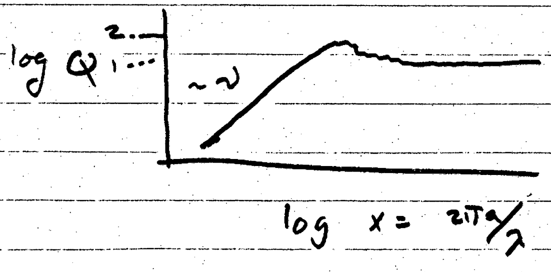

since $x_{opt\ prob} > 1 \Rightarrow X_{radio} > 1$ $a \gtrsim \dfrac{\lambda_{max}}{2\pi}$ (~ 2 cm)

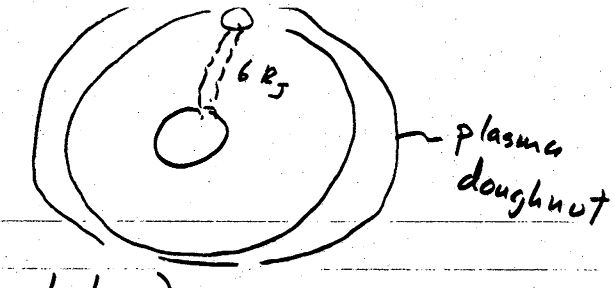

# IO

Low Frequency bursts (~10 MHz & below)
near higher end of freq rance "associated" with IO

For plasma emission ~~in~~ characteristic frequencies are

$$\nu_p \sim \left(\frac{n e^2}{m_e}\right)^{1/2} \quad \nu_c \sim \frac{eB}{mc} = 4\ \text{MHz/Gauss} \quad + \quad \nu_H = \sqrt{\nu_p^2+\nu_c^2}$$

$\sim 10\,\text{kHz} \cdot n^{1/2}$

$\sim$

at IO $B \sim 2 \cdot 10^{-2}$, $n \sim 4 \cdot 10^3$

$\nu_c \sim 80\,\text{kHz}$, $\nu_p \sim 500\,\text{kHz}$

at Jupiter ionosphere $B \sim 1\text{-}2$ $n \sim 10^{5-6}$

$\nu_{c\,H} \sim 10$ MHz

Connection by flux tube "exists" if

$$T_B = \frac{R}{V_A} < T_{diff\,IO} \approx 10^{3.4}\,\text{s}$$

$V_A \sim 300$ km s$^{-1}$ ; $T_B \sim 10^3$ s !

"Injection" by MHD waves
or accelerating e$^-$ in $\frac{V \times B}{c} \times R_{IO} = 500$ keV field
diffusion anisotropy
which stream down / up field lines

interact w/ plasma waves at bottom
via (coherent) maser type effect

especially if there are anisotropies in p,μ space

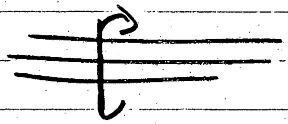

might explain beaming

Propagation problems

Titan?

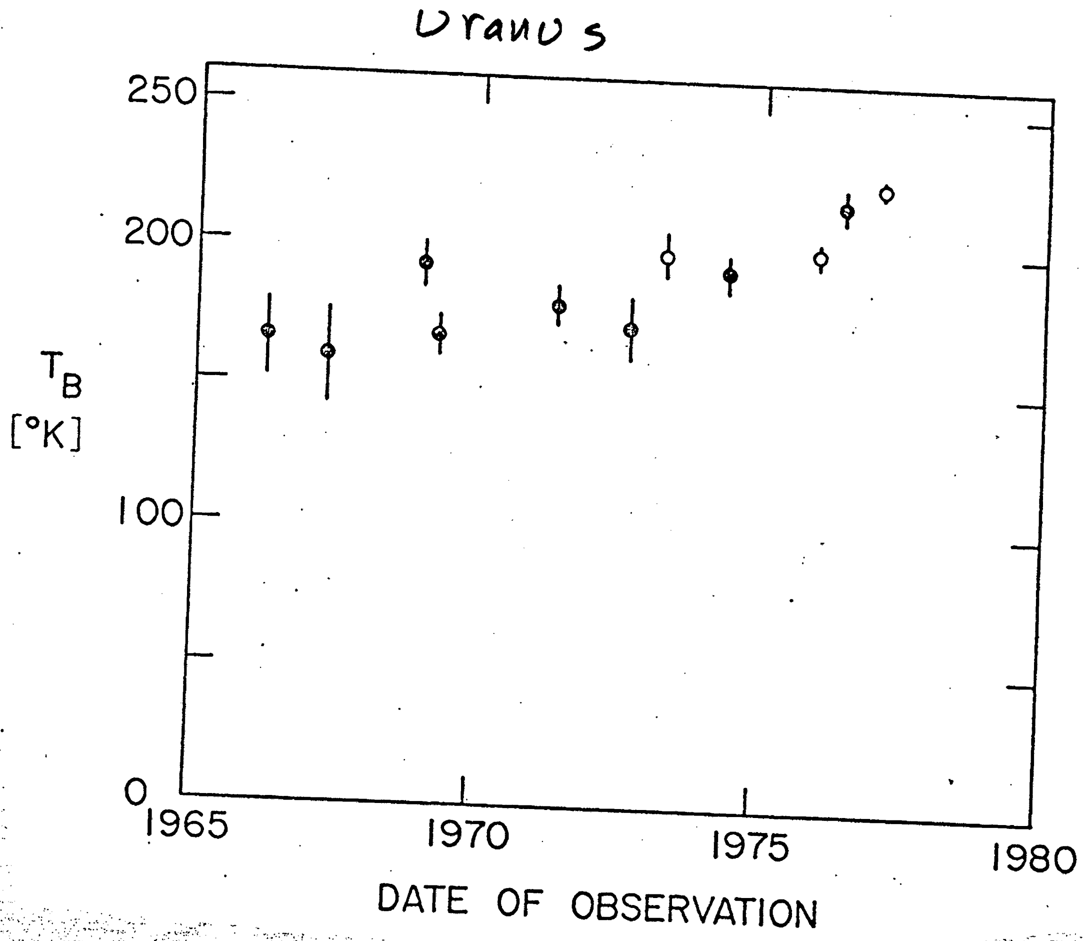

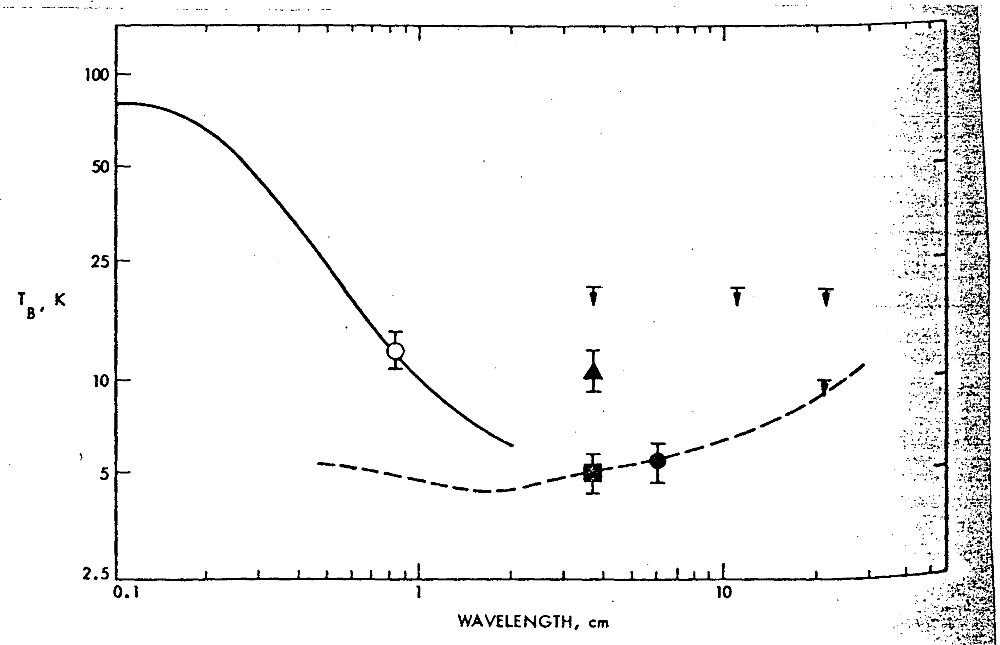

FIG. 9. The microwave spectrum of Saturn's rings. The present measurement is indicated by an open circle; others are due to Cuzzi and Dent (1975), ▲, Muhleman (1976), ■, and Jaffe (1977), ●. Upper limits of 20°K are given by Briggs (1974), at 3.7, 11, and 21 cm; and 10°K by Berge and Muhleman (1973), at 21 cm. The dashed curve indicates a possible spectrum due to reflection of the disk emission from the rings, and the solid curve shows the millimeter-wavelength spectrum of an ice model for the rings discussed in the text.

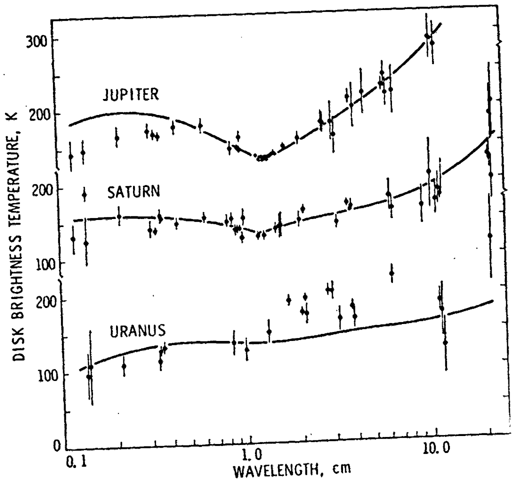

FIG. 2. Microwave spectra for Jupiter, Satur
and Uranus. The data shown have been compil
by us from measurements published in the op
literature and adjusted for flux density scale a
solid angle. The solid lines show our model cal
lations for deep convective $H_2$–He atmospheres
which $NH_3$ is uniformly mixed ($1.5 \times 10^{-4}$ mix
ratio) at depth and follows a saturation va
pressure in the upper atmosphere. At the 10-a
level, the corresponding temperatures are 354, 2
and 185°K for Jupiter, Saturn, and Uranus,
spectively. The Jupiter and Saturn data are c
sistent with the nominal model atmosphere calc
tions, whereas the Uranus data are not.

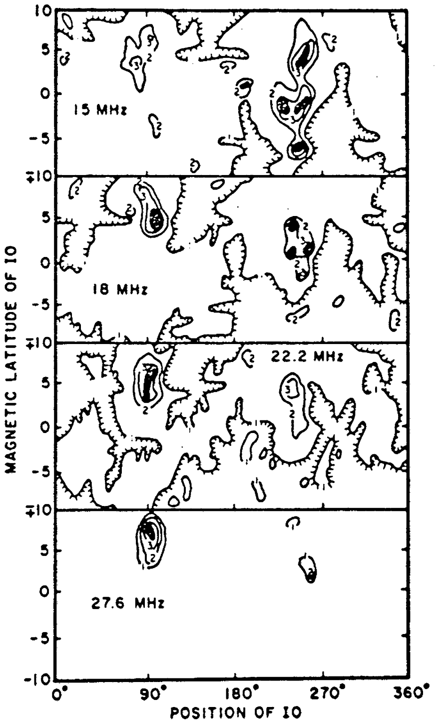

Fig. 6. Contours of relative flux at the same frequencies, for the same observing period, and in the same coordinate system as in Fig. 5. Contour "1" corresponds to a relative flux of 12.43, 16.22, 12.37, and $9.07 \times 10^{-20}$ W m$^{-2}$ MHz$^{-1}$ at 15, 18, 22.2, and 27.6 MHz, respectively.

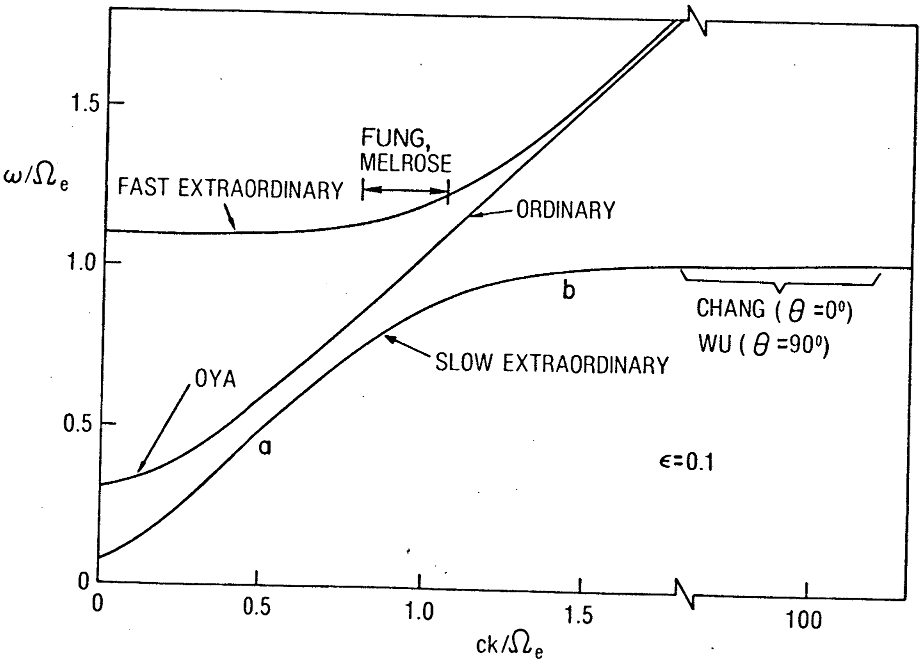

Fig. 8. Dispersion curves and indices of refraction of the ordinary and extraordinary modes for $\epsilon \ll 1$. The approximate regions of instability found by various authors are indicated.